

SIMULATION EXPERIMENT ON THE EFFECT OF HYDRODYNAMICS ON ALTERATION OF ORTHOCLASE UNDER RESERVOIR CONDITIONS

Yongwang ZHANG^{1,2} & Shanbin JIANG²

¹State Key Laboratory of Petroleum Resources and Prospecting, 18 Fuxue Road, Changping, Beijing 102249, China.
Email: zyw75@126.com

²College of Geosciences, China University of Petroleum-Beijing, 18 Fuxue Road, Changping, Beijing 102249, China.
Email: 13132103837@163.com

Abstract: The dissolution of feldspar is the main mechanism for the formation of secondary pores in deep sandstone reservoirs, which is controlled by pore fluid properties and fluid dynamics. The simulation experiment analyzed the effect of different fluid/rock ratios (hydrodynamics) on the orthoclase dissolution kinetics under reservoir diagenesis conditions. The experimental temperature was set at 100°C; the solutions were divided into acetic acid solutions and hydrochloric acid solutions, with pH values at 2 and 4; the reaction time was between 30 days and 80 days. The experimental results show that the fluid/rock ratio is an important factor controlling the feldspar dissolution. The higher the fluid/rock ratio, the stronger the fluid's ability to dissolve at orthoclase, and the more the release of Al and Si. With the increase of fluid/rock ratio, it is possible to observe more noticeable dissolution characteristics from the feldspar morphology. The lower the fluid/rock ratio, the higher the concentration of Al and Si ions released by orthoclase dissolution, and the easier it is to cause the precipitation of clay minerals, which is not conducive to the improvement of reservoir physical properties. The fluid/rock ratio is an important controlling factor on the formation and distribution of authigenic minerals such as kaolinite. The research results are of great implications in the feldspar dissolution to form secondary pores in the burial diagenesis process. In the sandstone-shale contacts or sandstone reservoirs with good initial physical properties, the strong fluid flow is conducive to the secondary pores formation. The experimental findings are helpful for us to understand better the process and mechanism of feldspar alteration and secondary pores formation.

Keywords: reservoir conditions, fluid/rock ratio, orthoclase dissolution, simulation experiment

1. INTRODUCTION

The quality of sandstone reservoir is largely controlled by its diagenetic history (Yang et al., 2020). The pore space is filled with the authigenic clay minerals, such as kaolinite and illite, it will significantly reduce the sandstone porosity and permeability (Nadeau, 1998). The dissolution of framework-grained feldspar minerals, however, forms secondary pores, which can increase the deep sandstone porosity (Schmidt & McDonald, 1979; Karner & Schreiber, 1993; Lanson et al., 2002). Under reservoir conditions, the quantity, dynamics and properties of the pore fluid are the key factors controlling the feldspar dissolution, so the fluid flow and fluid-rock reaction need to be correctly understood to improve the success rate of reservoir quality prediction (Zhong et al., 2003; Dutton,

2008; Dutton et al., 2012; Loyd et al., 2012; Wang et al., 2016; Lai et al., 2017). The diagenetic reaction cannot be observed explicitly within the deep sandstone reservoir. The diagenetic reaction must be analyzed using indirect methods, such as petrographic observation, experimental study, and diagenetic simulation. The mineral dissolution experimental study aims to understand the geochemical evolution of water-rock interaction better and to replicate the natural diagenetic process fully. Most chemical reactions that occur during diagenesis are mainly controlled by the reaction rate of mineral (Huang et al., 1986). Previous studies generally focused on the effects of fluid properties and mineral composition on feldspar alteration under reservoir conditions (Huang et al., 1992; Small et al., 1992; Karner et al., 1993; Benezeth et al., 1994; Kawano et al., 1995; Blake et al., 1996; Welch et al., 1996; Thyne, 2001). It has important

significance to study the effects of different fluid/rock ratios (hydrodynamics) on feldspar dissolution kinetics, clay mineral precipitation, secondary pore formation, and the diagenetic evolution of pore fluid through simulation experiments under reservoir burial diagenesis condition.

2. EXPERIMENTAL PROCEDURES

2.1 Experimental purpose

The effects of different hydrodynamics (fluid/rock ratios) on the orthoclase dissolution kinetics and the evolution of pore fluid are studied under the reservoir diagenesis condition, to reveal the formation mechanism of secondary pores. The experiment is a static experiment that simulates the strength of the pore fluid hydrodynamics by changing the reaction solution's fluid/rock ratio to the feldspar sample.

2.2 Experimental samples and experimental method

2.2.1 Starting feldspars

The orthoclase samples were taken from the Institute of Mineral Deposits, Chinese Academy of Geological Sciences. The sample was crushed to 100 mesh and washed with deionized water. The X-ray powder diffraction (XRD) analysis of the sample showed that the mineral composition was 83.8% of orthoclase and 16.2% of plagioclase (Fig. 1). To remove the fine particles on the feldspar surface, the feldspar sample was washed with acetone solution ultrasonic wave multiple times before the reaction until the

suspension was clean. To compare with the sample after the reaction, we observed the surface of feldspar, which was clean before the reaction by a scanning electron microscope. The results showed that the feldspar particle surface was smooth, without ultra-fine particles or obvious alteration characteristics, and many particles had angular surface defects caused by mechanical separation (Fig. 6).

2.2.2 Starting solutions

The fluid samples used in the experiment were the aqueous solutions of acetic acid or hydrochloric acid chemical reagents with distilled deionized water, and the pH values were set to 2 and 4. We adjusted the pH values of the solutions by adding acetic acid or hydrochloric acid into deionized water. See Table 2 for the compositions of starting solutions.

2.2.3 Experimental apparatus and method

The apparatus of the simulation experiment was a high-temperature and high-pressure reactor consisting of an inner cup polytetrafluoroethylene and a jacket of stainless steel with a temperature of approximately $\leq 230^{\circ}\text{C}$ and pressure ≤ 3 MPa. The experimental temperature was set to 100°C , and the corresponding saturated vapor pressure was the pressure (Table 1). Through the analysis of groundwater in 15 oil and gas fields in the United States, Carothers & Kharaka (1979) found that the main type of acids in oil field water are organic acids, and the temperature range of the maximum concentration of organic acids is 80°C – 130°C . Organic acids can be destroyed by microbial

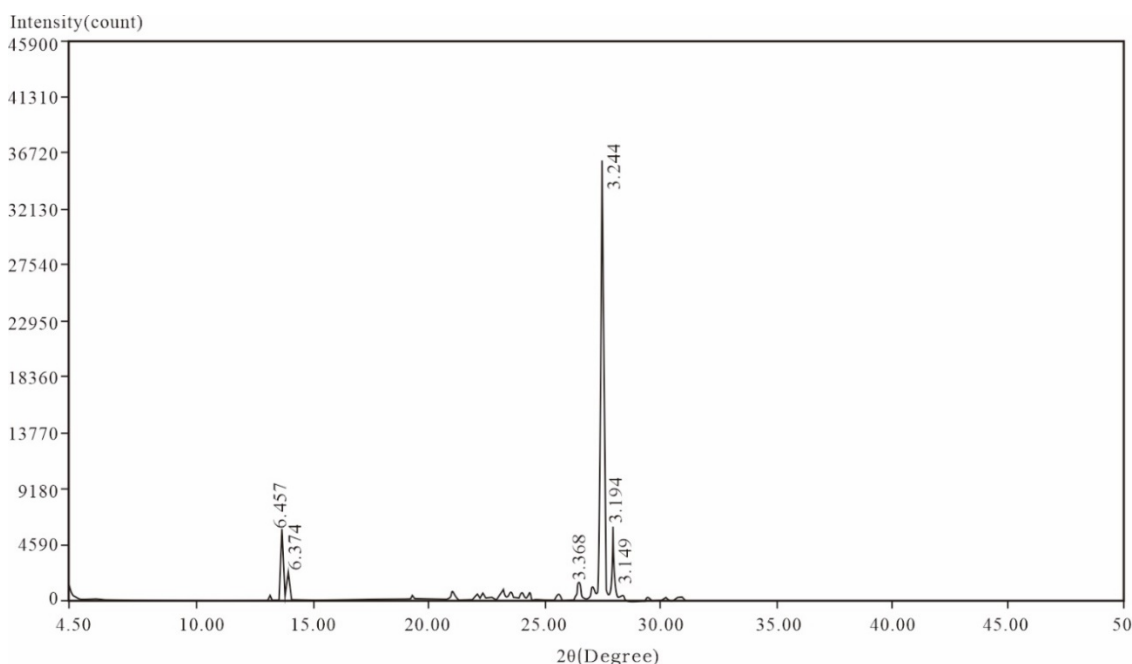


Figure 1. XRD analysis results of feldspar samples.

bacteria at lower temperatures. Organic acids will decarboxylate at higher temperatures to form methane and CO₂, so the experimental temperature was set at 100°C, which was consistent with the best temperature for the existence of the organic acid. The pH value is a significant controlling factor on the feldspar dissolution rate (Lasaga, 1984). A pH value of 4 was chosen to represent the average acidic formation water. The pH=2 was chosen to compare the effect of solution acidity on feldspar dissolution and to speed up the reaction. Although the extremely acidic solution of pH=2 cannot be sustained for a long time, in the natural diagenetic environment, the entry of mudstone acidic water into sandstone during compaction and montmorillonite illitization will reduce the pH value of formation water (Mansurbeg et al., 2008). The effect of pressure on the rate of mineral dissolution has not been documented, but the smallest effect is considered at the experimental temperature of 100°C (Surdam & Crossey, 1985).

The running time of the experiment ranged from 30 days to 80 days. After the end of the reaction, the reaction container was cooled for 30 minutes, and the solution was filtered with 0.22- μ m filter paper. After centrifugation, the ionic analyzes of K, Al, Si etc. were conducted for the fluid sample. The alteration characteristics and authigenic minerals of feldspar samples were observed by SED and XRD.

3. ANALYZES AND TESTING METHODS

3.1 XRD analyzes and testing

Semiquantitative bulk-rock XRD analysis and clay fraction XRD analysis were carried out in D/max-2500 diffractometer equipped with Cu(K α) radiation

(30 kV, 20 mA) and a nickel filter in oriented samples that were air-dried. The laboratory temperature and humidity were 26°C and 30% RH, respectively. According to the Stokes sedimentation theorem in hydrostatics, clay mineral samples with particle size < 10 μ m and < 2 μ m were extracted by water suspension separation or centrifugal separation, respectively. The clay mineral samples with particle size less than 10 μ m were used to determine the total relative content of clay minerals in the original rock. Clay mineral samples with particle size < 2 μ m were used to determine the relative content of various clay mineral species.

3.2 Scanning electron microscopy (SEM)

A Quanta 200F scanning electron microscopy (SEM) was used to analyze the secondary precipitates and orthoclase corrosion signs equipped with energy-dispersive spectroscopy (EDS). All samples were coated with a thin layer of gold prior to examination. Under a high vacuum, the secondary electron imaging resolution is 2 nm, and the backscattered electron imaging resolution is 2.5 nm. The electron images were taken with an acceleration voltage of 30 kV. The magnifications under a high vacuum are 12X ~ 1,000,000X.

3.3 Fluid analyses and testing methods

The experimental apparatus was an inductively coupled plasma emission spectrometer. The laboratory room temperature was 20°C, and the humidity was 2%–45%. The multi-element mixed standard solution was determined, with repeated RSD determination for ten

Table 1. Feldspar dissolution experiments

Run No.	Fluid			Experiment conditions		
	pH (Acid type)	Salinity (mol/l)	Fluid/rock	volume (ml)	temperature (°C)	React time (day)
P1	2.0 (acetic acid)	1 mol KCl	100	100	100	80
P 2	2.0 (acetic acid)	0	100	100	100	
P 3	2.0 (acetic acid)	0	50	50	100	
P 4	2.0 (acetic acid)	0	20	20	100	
P 5	2.0 (acetic acid)	0	100	100	100	
P 6	2.0 (acetic acid)	0	50	50	100	45
P 7	2.0 (acetic acid)	0	20	20	100	
P 8	2.0 (acetic acid)	0	100	100	100	
P 9	2.0 (acetic acid)	0	50	50	100	30
P 10	2.0 (acetic acid)	0	20	20	100	
P 11	2.0 (acetic acid)	0	10	10	100	
P 12	2.0 (acetic acid)	0	50	50	100	
P 13	2.0 (acetic acid)	0	20	20	100	
P 14	2.0 (acetic acid)	0	10	10	100	
P 15	4.0 (acetic acid)	0	50	50	100	
P 16	4.0 (acetic acid)	0	20	20	100	

times less than 0.5% and experimental apparatus error at 1%–5%. The system washing solution was determined as the reference value for the solution to be tested before testing the sample. Each sample was rinsed with a system washing solution before analysis until the test probe reached the lowest new strength, and sample analysis started after the analysis signal was stable. In the process of sample measurement, the sample should be diluted and re-determined if the concentration of elements to be measured in the sample exceeded the range of the standard curve. After the solution test was completed, the results were corrected according to the concentration of each ion in the system washing solution.

4. RESULTS AND DISCUSSION

Four kinds of fluid/rock ratios were used to evaluate the alteration characteristics and mechanism of orthoclase in acid solution under different fluid/rock ratios: 10 ml/g, 20 ml/g, 50 ml/g, and 100 ml/g. The experimental solutions were basically acetic acid solutions at pH=2. In order to compare the effect of pH and fluid salinity on feldspar dissolution, a solution with pH 4 and KCl was also set. The dissolution rate of feldspar in aqueous solution is generally expressed by changing the concentration of dissolved ions over time. Because different fluid/rock ratios were set, when the quality of the solid sample was fixed, the amount of solution used was different; therefore, the quantity of ions released from feldspar in a certain time was used to

express the dissolution rate (dc_i/dt). The solubility of most rock-forming minerals was lower than 10^{-6} mol/L, and the dissolution was controlled by the reaction rate at the interface between minerals and solution.

$dc_i/dt = \frac{A}{V} \cdot v_i \cdot k$ (A represents the surface area of feldspar; V represents the solution volume; V_i represents the content of chemical component i in orthoclase, in which Si = 3, K = 1, and Al = 1) (Lasaga, 1984).

4.1 Changes in fluid composition (K, Al, and Si)

The analytical data for the fluid composition is listed in Table 2. The concentration of Al and Si decreased over a certain reaction time with the increase of fluid/rock ratio (Fig. 2). Since the contact area of the solution to feldspar was higher when the fluid/rock ratio was low, and the concentration would reach a certain level in a shorter time (Aagard & Helgeson, 1982).

Because the volumes of the solutions used in the experiment with different fluid/rock ratios were different, the concentration of the solution could not be used to explain the rate of feldspar dissolution. The rate of dissolution of orthoclase in aqueous solution was expressed in a given time by the number of free dissolved cations. The concentrations of feldspar components K, Al, and Si were converted into net total release (Table 3). The higher the cation content in the solution is, the higher the degree of feldspar alteration is. The changes of ion release amount under different

Table 2. Fluid chemistry data of experiment($\mu\text{g/mL}$)

Run No.	Na	Ca	K	Al	Si
L1	7.6973	2.7839	2.1923	< 0.0000	1.6941
L2	5.5867	2.6842	1.9938	< 0.0000	0.6913
L3	4.7247	3.6448	2.2749	< 0.0000	0.7184
L4	8.6243	2.886	346.0261	< 0.0000	1.4522
P1	48.3189	19.6634	35.1342	11.286	32.9702
P 2	3.1457	2.6739	47.9324	23.1245	58.8537
P 3	4.1254	4.3264	41.4862	22.1247	69.9516
P 4	10.3577	16.2611	47.9335	28.71	91.5569
P 5	4.4273	14.4617	36.9655	10.1778	61.7637
P 6	7.4272	5.0674	28.0233	13.1454	66.4304
P 7	7.1259	17.5796	70.7933	22.9839	72.8108
P 8	7.5432	7.8356	58.5902	9.1676	28.9389
P 9	2.8652	17.195	42.9312	17.2862	53.1676
P 10	2.6897	32.6305	30.2933	23.5863	66.4119
P 11	7.1605	12.8019	66.7664	22.2712	70.8933
P 12	10.3756	14.6866	69.1736	26.3366	86.2331
P 13	5.1618	17.5974	46.721	19.0501	60.7813
P 14	3.0237	4.6118	86.374	13.1605	42.7068
P 15	0.0511	15.313	70.5051	1.3056	10.9797
P 16	4.1383	3.3907	19.5741	0.5303	4.5852

L1: pH=2.0 (acetic acid + deionized water); L2: pH=4.0(acetic acid + deionized water);

L3: pH=2.0(hydrochloric acid + deionized water); L4: pH=2.0 (acetic acid + deionized water +0.01 MKCL)

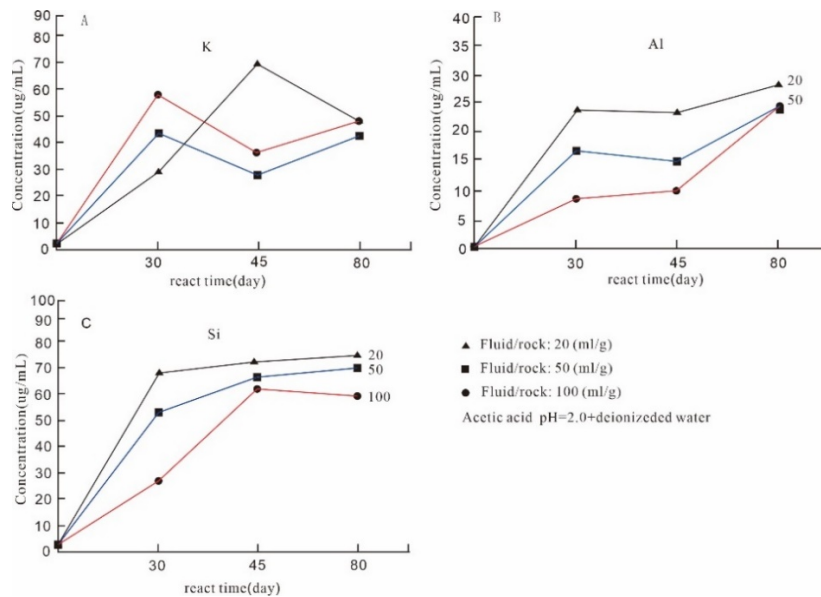


Figure 2. The concentrations of three kinds of ions (K, Al, Si) under different fluid/rock ratios as a function of time.

Table 3. Net release of the element (release rate) (mg)

Run No.	Na	Ca	K	Al	Si
P1	4.8319	1.9663	3.5134	1.1286	3.2970
P 2	0.3146	0.2674	4.7932	2.3125	5.8854
P 3	0.2063	0.2163	2.0743	1.1062	3.4976
P 4	0.2072	0.3252	0.9587	0.5742	1.8311
P 5	0.4427	1.4462	3.6966	1.0178	6.1764
P 6	0.3714	0.2534	1.4012	0.6573	3.3215
P 7	0.1425	0.3516	1.4159	0.4597	1.4562
P 8	0.7543	0.7836	5.8590	0.9168	2.8939
P 9	0.1433	0.8598	2.1466	0.8643	2.6584
P 10	0.0538	0.6526	0.6059	0.4717	1.3282
P 11	0.0716	0.1280	0.6677	0.2227	0.7089
P 12	0.5188	0.7343	3.4587	1.3168	4.3117
P 13	0.1032	0.3519	0.9344	0.3810	1.2156
P 14	0.0302	0.0461	0.8637	0.1316	0.4271
P 15	0.0026	0.7657	3.5253	0.0653	0.5490
P 16	0.0828	0.0678	0.3915	0.0106	0.0917

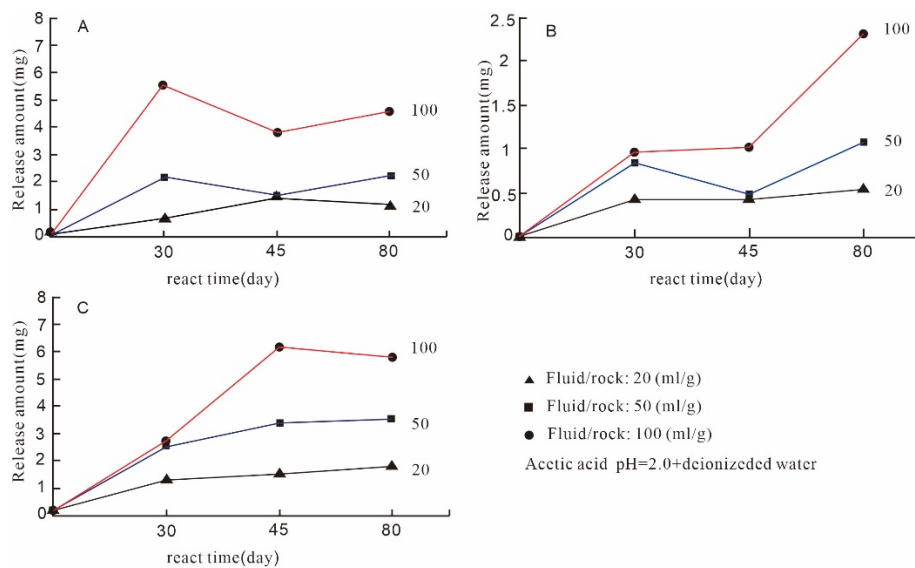


Figure 3. The total release of three kinds of ions (K, Al, Si) under different fluid/rock ratios as a function of time

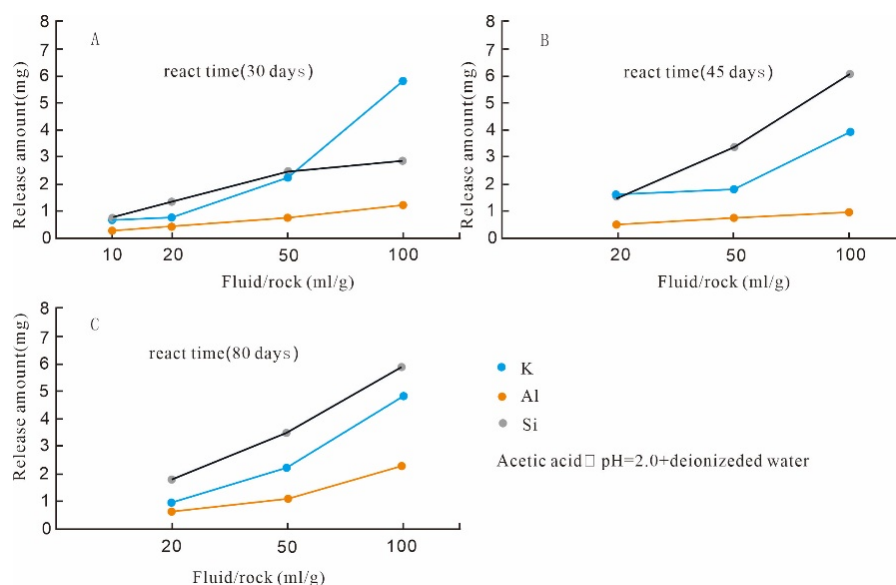


Figure 4. Comparative characteristics of the total release of three ions (K, Al, Si) under different fluid/rock ratios

fluid/rock ratios of 30 days, 45 days, and 80 days were summarized, respectively (Fig. 3). With the increase of fluid/rock ratio, the release amount of Al and Si ions increased, indicating that the reaction solution with a higher fluid/rock ratio had a stronger ability to dissolve ions. The reaction solution with a lower fluid/rock ratio had a weaker ability to dissolve ions. With the increase of dissolved cation concentration in aqueous solution, the feldspar dissolution will be inhibited, resulting in a slower dissolution rate of feldspar. Figure 4 shows the effect of the fluid/rock ratio on feldspar dissolution rate. The feldspar dissolution product Al has very low solubility, and the concentration of Al in oil field water is only a few ppm (Stoessell & Pittman, 1990b), which is the most stable element in feldspar dissolution products. The experimental results show that the solubility of Al increases with the increase of fluid/rock ratio (Fig. 4). The concentration of Al in aqueous solution is the Al activities indicator. Therefore, the migration and enrichment of feldspar dissolution product Al are related to pore fluids geochemistry, hydrodynamics, and diagenetic temperature (Mansurbeg et al., 2008).

The chemical reaction at the interface between the minerals and the solution is presumed to control the dissolution of feldspar without forming a leached layer. The quantity of elements dissolved and released from feldspar is in proportion to the chemical reaction formula, i.e., consistent isochemical reaction (Lasaga, 1984), when the feldspar is far from equilibrium. Different from the results of previous studies, although the release of K and Al is lower than that of Si in general, it is not a consistent isochemical reaction. If orthoclase is consistently dissolved, K, Al and Si have to be in the molecular formula according to the proportion of chemical composition. Every time the 1

mol K and Al are released, the 3 mol Si is released. It may be related to the presence of a certain amount of plagioclase in the sample. At the same time, Al in potash feldspar is not preferentially complexed by organic acids, resulting in the faster release. The solubility of feldspar is greatly affected by the pH value of the solution. For acetic acid solutions with pH values of 2 and 4, a decrease in pH of 2 increases the number of dissolved ions by an order of magnitude (Table 3). Since it is not a buffer solution, the pH value of the solution will change with the progress of the reaction, so the complexation of organic acids is difficult to compare. The experimental results show that orthoclase goes through an early linear rapid dissolution stage under different fluid/rock ratios, and the stage with a fast dissolution rate will last for several hours or days (Chou & Wollast, 1984). After the early rapid release stage, orthoclase reached the non-linear release stage, the solute concentration started to reach equilibrium, and the release of elements would be slower, which may be due to the formation of secondary minerals, the presence of high energy points on the surface of orthoclase, or a change in the solution composition. The initial release rate is similar to the actual release rate, which is correlated with the fluid/rock ratio and ion concentration. The experimental findings support the surface reaction model of mineral dissolution. According to the surface reaction model, the release rate of feldspar component has a strong relationship with the concentration of solution. The dissolution of orthoclase can achieve a higher concentration faster under the condition of a higher fluid/rock ratio (Fig. 2) than under the condition of a lower fluid/rock ratio, so it has a slower release rate. In the case of a fluid/rock ratio of 20, after 30 days of feldspar dissolution, Al and Si reached an

equilibrium state, which may be due to the increase of dissolution products leading to the emergence of metastable solid-phase precipitation (Velbel, 1986).

The changing characteristics of fluid composition reveal that the lower the fluid/rock ratio, the higher the concentration of feldspar dissolved components, which leads to the easier precipitation of clay minerals. By comparing the acetic acid solution with and without KCl, it can be seen that the amount of K, Al and Si released by the dissolution of potassium feldspar after the addition of KCl in the solution decreases correspondingly (Fig. 5, Table 3), indicating that the ion concentration affects the dissolution rate of feldspar, which is also in line with the feldspar dissolution surface model.

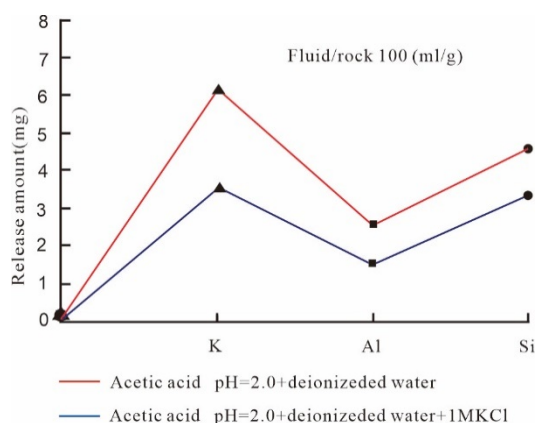


Figure 5. Effect of salinity on feldspar dissolution

4.2 Changing characteristics of feldspar samples

We used scanning electron microscope to observe the visible dissolution marks and secondary precipitates of the feldspar samples before and after the reaction. After detailed observation of the feldspar samples after the reaction, the feldspar was sufficiently dissolved only in the experiment with a fluid/rock ratio of 100, showing an obvious dissolution sign. It is consistent with the dissolution characteristics explained by the change of fluid composition. The greater the fluid/rock ratio is, the higher the dissolution degree of feldspar is. Figure 6 shows the dissolved feldspar. The feldspar in the fluid/rock ratio of 20 experiment has a slight dissolution trace, but the feldspar in the fluid/rock ratio of 100 experiment has serious alteration, and almost every particle shows the characteristics of alteration. These alteration characteristics are similar to those of feldspar in the sandstone reservoir of Shahejie Formation in Dongying Sag (Zhang et al., 2015). Feldspar dissolution starts from the surface of the cleavage and has prismatic corrosion pits, which often grow along with two groups of cleavage directions. This

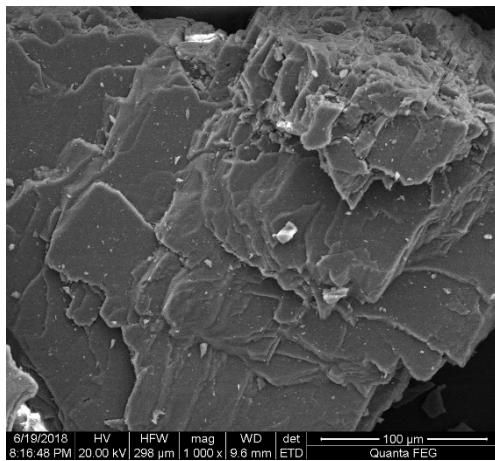
dissolution structure shows feldspar dissolution and the transport of Al and Si within the solution. With the increase of fluid/rock ratio, it can be seen from the morphology of feldspar that the alteration degree of feldspar increases (Fig. 6). It shows that with the increase of hydrodynamics and pore fluid flow, the dissolution of feldspar is enhanced, while the concentration of Al and Si decreases, which is conducive to the secondary pores formation. The secondary precipitates in stable and metastable states in the experiment may be due to the absence or a very small proportion, so it is difficult to observe by XRD.

4.3 Diagenetic implications

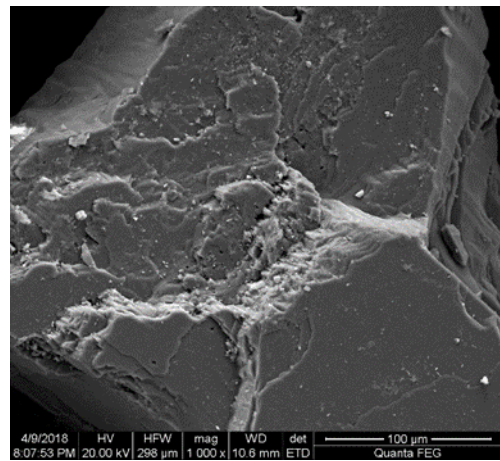
The fluid/rock ratio has important effect on feldspar dissolution and the formation of secondary pores in sandstone reservoirs and the geochemical evolution of pore fluids. The release rate of feldspar components for deep sandstone reservoirs is related to the ratio of total fluid volume to the surface area of pores in the rock (Thyne et al., 2001). The experimental results show that the higher the fluid/rock ratio, the higher the release rate of feldspar, so the larger the secondary pores are formed. Clay minerals are also formed when feldspar dissolves. The formation of clay minerals is controlled by the dissolved ions concentration in the solution, and the higher the concentration, the more likely precipitation will occur. The higher the fluid/rock ratio, the lower the ion concentration in the solution, and the fewer clay minerals precipitated, which is more conducive to the feldspar dissolution and secondary pores formation. For sandstone reservoirs, fluid properties and fluid dynamics (fluid/rock ratio) control the dissolution of feldspar. Under the high hydrodynamics conditions, the unsaturated fluid can dissolve more minerals, at the same time, it can take away the dissolved products and precipitate fewer clay minerals, which is helpful to improve the porosity and permeability of the reservoir. In the sandstone-shale contacts and sandstone with excellent initial physical properties, the fluid flow is active, which is conducive to the secondary pores formation. With the increase of fluid/rock ratio, the release amount of Al increases, and the concentration decreases.

Therefore, the migration and enrichment of feldspar dissolution product Al are related to pore fluid geochemistry, hydrodynamics, and diagenetic temperature. The fluid/rock ratio has important effect on the formation and distribution of authigenic minerals such as kaolinite.

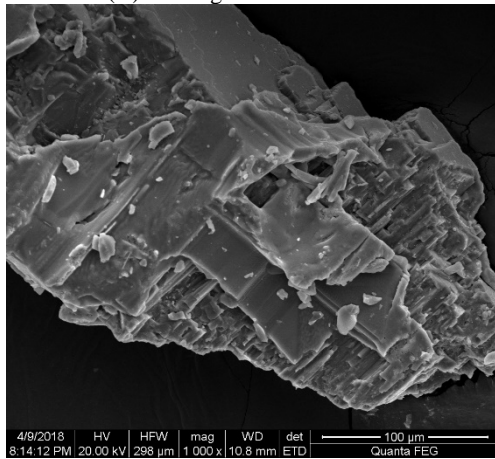
Although the data from the experimental study of single mineral dissolution cannot be directly applied to the natural diagenetic system, it can improve our understanding of the diagenetic process.



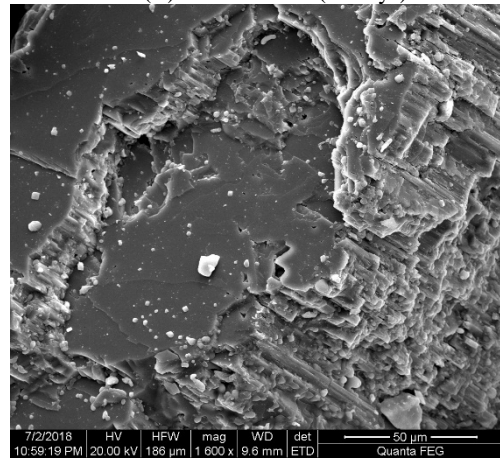
(A) Starting material



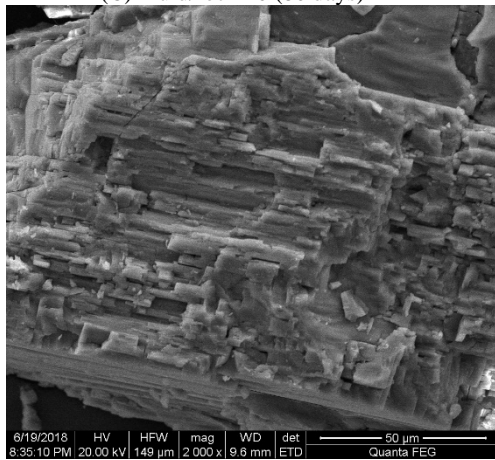
(B) Fluid/rock 20 (30 days)



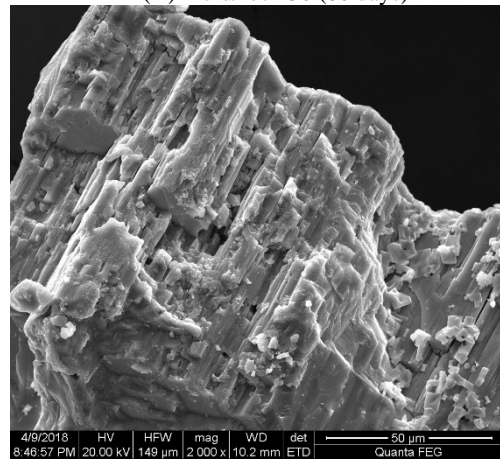
(C) Fluid/rock 20 (80 days)



(D) Fluid/rock 50 (80 days)



(E) Fluid/rock 100 (50 days)



(F) Fluid/rock 100 (80 days)

Figure 6. The dissolution characteristics of feldspar under different fluid/rock ratios

5. CONCLUSIONS

Fluid/rock ratio is an important controlling factor on feldspar dissolution and is of great significance for the formation of secondary pores in sandstone reservoirs and the geochemical evolution of pore fluids.

With the increase of fluid/rock ratio, the dissolution rate of Al and Si of orthoclase increases, which shows that the dissolution of orthoclase is mainly controlled by the surface reaction model of mineral dissolution, and the releasing rate of dissolved components is related to the ion concentration in the solution. Through the scanning electron microscope observation of feldspar samples before and after the reaction, it is revealed that the

higher the fluid/rock ratio, the stronger the dissolution of feldspar.

The dissolution rate of Al and Si of orthoclase decreases with the decrease of fluid/rock ratio, but the concentration of Al and Si increases, leading to more precipitation of clay minerals, thus it is not conducive to improving the porosity and permeability of the reservoir.

The solubility of Al has important effect on the dissolution rate of feldspar, and the increase of fluid/rock ratio can improve the solubility of Al, so the fluid/rock ratio is an important factor to control the formation and distribution of authigenic minerals such as kaolinite.

Acknowledgments

This work was supported by National Natural Science Foundation of China (grant No. 41572113).

REFERENCES

- Aagard P. & Helgeson H.C.** 1982. *Thermodynamic and kinetic constraints on reaction rates among mineral and aqueous solutions*, I. Theoretical considerations. *Am. J. Sci.*, 282, 237-285.
- Benezeth, A., Castet, S., Dandurand, J., Gout, R. & Schott, J.** 1994. *Experimental study of aluminum-acetate complexing between 60 and 200°C*, *Geochimica et Cosmochimica Acta*, 58(21), 4561-4571.
- Blake, R.E. & Walter, L.M.** 1996. *Effects of organic acids on the dissolution of orthoclase at 80°C and pH 6*, *Chemical Geology*, 132, 91-102.
- Carothers, W.W. & Kharaka, Y.K.** 1979. *Organic Acid Anions in Oil-Field Waters and Origin of Natural Gas*: abstract. *AAPG Bulletin*, 63, 428-429
- Chou, L. & Wollast, R.** 1984. *Study of the weathering of albite at room temperature and pressure with a fluidized bed reactor*, *Geochim. Cosmochim. Acta*, 48, 2205-2217.
- Dutton, S.P.** 2008. *Calcite cement in Permian deep-water sandstones, Delaware Basin, west Texas: origin, distribution, and effect on reservoir properties*, *AAPG Bulletin*, 92, 765-787.
- Dutton, S.P., Loucks, R.G. & Day-Stirrat, R.J.** 2012. *Impact of regional variation in detrital mineral composition on reservoir quality in deep to ultradeep lower Miocene sandstones, western Gulf of Mexico*, *Marine and Petroleum Geology*, 35, 139-153.
- Thyne G.** 2001. *A model for diagenetic mass transfer between adjacent sandstone and shale*. *Marine and Petroleum Geology*, 18: 743-755.
- Huang, W. L.; Bisshop, A. M. & Brown, R. W.** 1986. *The effect of fluid/rock ratio on feldspar dissolution and illite formation under reservoir conditions*, *Clay Minerals*, 21, 585-601.
- Huang, W.L. & Longo, J.M.** 1982. *The effect of organics on feldspar dissolution and the development of secondary porosity*, *Chemical Geology*, 98, 271-292.
- Karner, S.L. & Schreiber, B.C.** 1993. *Experimental simulation of plagioclase diagenesis at P-T conditions of 3.5 km burial depth*, *Pure and applied geophysics*, *Pure and applied geophysics* 141(2), 221-247.
- Kawano, M. & Tomita, K.** 1995. *Formation of mica during experimental alteration of K-feldspar*, *Clays and Clay Minerals*, 43(4), 397-405.
- Lai, J.; Wang, G.; Wang, S., Cao, J., Li, M., Pang, X., Zhou, Z., Fan, X., Dai, Q. & Liu, Y.** 2018. *Review of diagenetic facies in tight sandstones: Diagenesis, diagenetic minerals, and prediction via well logs*, *Earth-Science Reviews*, 185: 234-258.
- Lanson, B., Beaufort, D. & G. Berger, D.** 2002. *Authigenic kaolin and illitic minerals during burial diagenesis of sandstones: a review*, *Clay Minerals*, 37, 1-22.
- Lasaga, A.C.** 1984. *Chemical kinetics of water-rock interactions*, *Journal of Geophysical Research: Solid Earth*, 89(B6), 4009-4025.
- Loyd, S.J.; Corsetti, F.K.; Eiler, J.M. & Tripathi, A.K.** 2012. *Determining the diagenetic conditions of concretion formation: assessing temperatures and pore waters using clumped isotopes*, *Journal of Sedimentary Research*, 82, 1006-1016.
- Mansurbeg, H., Morad, S., Salam, A., Marfil, R., El-Gha, A., Nystuen, J.P., Caja, M.A., & Amorosi, A.** 2008. *Diagenesis and reservoir quality evolution of palaeocene deep-water, marine sandstones, the Shetland-Faroes Basin, British continental shelf*, *Marine and Petroleum Geology*, 25, 514-543.
- Nadeau P. H.** 1998. *An experimental study of the effects of diagenetic clay minerals on reservoir sands*, *Clays and Clay Minerals*, 46(1):18-26.
- Schmidt, V. & McDonald, D.A.** 1979. *The role of secondary porosity in the course of sandstone diagenesis*, *Soc. Econ. Paleontol. Mineral., Spec. Publ.* 26, 175-207.
- Small, J.S., Hamilton D.L. & Habesch, S.** 1992. *Experimental simulation of clay precipitation within reservoir sandstones 1: techniques and examples*, *Journal of sedimentary petrology*, 62(3), 508-519.
- Stoessell, R.K. & Pittman, E.D.** 1990b. *Secondary porosity revisited: The chemistry of feldspar dissolution by carboxylic acids anions*, *AAPG Bulletin*, 74(12), 1795-1805.
- Surdam, R.C. & Crossey, L.J.** 1985. *Organic-inorganic reactions during progressive burial: key to porosity and permeability enhancement and preservation*, *Philosophical Transactions of the Royal Society, London, Series A*, 315: 135-156.
- Surdam, R.C., Boese, S.W. & Crossey, L.W.** 1984. *The chemistry of secondary porosity*. In: McDonald, D.A., Surdam, R.C., (Eds.), *Clastic Diagenesis: American Association of Petroleum Geologists*

Memoir, 37, 127–134.

- Thyne, G., Boudreau, B.P.; Ramm, M. & Midtbo, R.E. et al.** 2001. *Simulation of potassium feldspar dissolution and illitization in the Statfjord Formation, North Sea*, AAPG Bulletin, 85(4), 621–635.
- Velbel, M.A.** 1986. *Influence of surface area, surface characteristics, and solution composition on feldspar weathering rates*. In *Geochemical Processes at Mineral Surfaces*. J. A. Davis and K. F. Hayes, eds. Washington, DC: American Chemical Society, 615-634.
- Wang, J.; Cao, Y.; Liu, K., Liu, J., Xue, X. & Xu, Q** 2016. *Pore fluid evolution, distribution and water-rock interactions of carbonate cements in red-bed sandstone reservoirs in the Dongying depression, China*, Marine and Petroleum Geology, 72, 279-294.
- Welch, P. A. & Ullman, W. J.** 1996. *Feldspar dissolution in acidic and organic solutions: Compositional and pH dependence of dissolution rate*, *Gewbimica et Cosmochimica Acta*, 60(16), 2939-2948.
- Yang, T., Cao, Y. & Friis, H.** 2020. *Diagenesis and reservoir quality of lacustrine deep-water gravity-flow sandstones in the Eocene Shahejie Formation in the Dongying sag, Jiyang depression, eastern China*, AAPG Bulletin, 104(5), 1045-1073.
- Zhang, Y.W., Zeng, J.H. & Qu, Z.Y.** 2015. *Development characteristics and genetic mechanism of authigenic kaolinite in sandstone reservoirs of the Dongying Sag, Bohai Bay Basin*, *Oil and Gas Geology*, 36(1), 73-79.
- Zhong, G.F.; Ma, Z.T.; Liu, R. L. & Wu, N.F.,**—2003. *Distribution of upper Cenozoic carbonate-cemented sandstones, Kuche depression, northwest China: insights from high-resolution borehole micro-resistivity imaging*, *Journal of Sedimentary Research*, 73(2), 177-186.

Received at: 05. 10. 2020

Revised at: 19. 02. 2021

Accepted for publication at: 22. 02. 2021

Published online at: 25. 02. 2021